Abstract

Diabetes mellitus is a chronic and severe disease that affects millions of people worldwide, including a significant number in India. Type-2 diabetes often leads to chronic non-healing wounds, causing significant problems for individuals' mobility and quality of life. Sitagliptin phosphate is an oral medication commonly used to treat these diabetic wounds. In this study, we aimed to optimize a transferosome hydrogel containing sitagliptin phosphate for better transdermal delivery of the drug. We used a Box-Behnken design, employing the rotary evaporation-sonication method to prepare the transferosome nanoparticles, and a three-factor, two-level factorial design for optimization. The factors tested were phospholipid concentration, surfactant concentration, and sonication time, while the dependent variables were entrapment efficiency and vesicle size. The optimized transferosome suspension was then used to prepare chitosan-PEG hydrogels loaded with silver nanoparticles (AgNPs). Higher phospholipid and surfactant concentrations increased entrapment efficiency, while surfactant concentration and sonication time reduced vesicle size. Morphological analysis revealed smooth, spherical, and uniform nanoparticles with pores and channels on their surface. The hydrogels exhibited uniform drug distribution and optimal spreadability. Hydrogels with a cross-linker showed improved swelling and controlled drug release. Stability tests conducted over 90 days indicated that the transferosome hydrogels maintained their properties. The dissolution rate of the drug from both the transferosomes and the transferosome hydrogel was rapid initially but prolonged over 12 hours. The study demonstrated the successful formulation of sitagliptin phosphate-loaded transferosome nanoparticles and transferosome hydrogel, which achieved the desired sustained-release profile. This sustained-release system has the potential to create a subcutaneous drug reservoir, improving patient safety and comfort. The findings suggest potential clinical applications for the transferosome nanoparticles and transferosome-loaded hydrogel.

1. Introduction

Diabetes mellitus is a chronic and severe illness that affected 462 million adults worldwide in 2017 representing 6.28% of the global population (Khan et al., 2020) and 77 million individuals in India in 2019 (Pradeepa and Mohan, 2021). Complications of diabetes can pose a threat to health and life if they are not effectively managed. There are several complications associated with diabetes, but pressure ulcers are a significant one, resulting in substantial morbidity, financial burdens, and decreased survival rates, along with reduced quality of life (Jan et al., 2013). Furthermore, diabetic patients are most likely to require amputations due to non-healing ulcers (Faglia et al., 2013). Type-2 diabetics suffer from chronic non-healing wounds that greatly impact their mobility and quality of life. Current clinical treatments do not work on these wounds, which lead to repeated amputations of peripheral limbs (Zhou et al., 2011). Wound healing occurs naturally through the spontaneous growth and regeneration of skin tissues, which restores the structural

integrity of damaged skin. Hemostasis, inflammation, angiogenesis, fibroblast proliferation, and tissue remodeling are all part of this intricate process (Ayello and Cuddigan, 2004; Eming et al., 2014). Diabetes patients, however, are more likely to suffer chronic wounds resulting from even minor trauma to parenchymal cells and stromal structures (Trengove et al., 1999). Chronic wounds are prone to repeated infections, prolonged inflammation, and impaired epidermal response to stimuli (Attinger et al., 2006; Stojadinovic et al., 2008; Woo et al., 2007).

Wound healing is impaired in diabetics due to a variety of factors, including biochemical, vascular, and neuropathic components (Greenhalgh, 2003). Having high blood sugar levels (hyperglycemia) leads to stiffened blood vessels, slower circulation, and dysfunctional microvasculature, resulting in reduced oxygen delivery to tissues (Dinh et al., 2011). Diabetes also contributes to diminished white blood cell migration into wounds, making them more susceptible to infections as a result of changes to blood vessels (Greenhalgh, 2003). White blood cells can also be compromised by a hyperglycemic environment. The chronicity of wounds that go unnoticed and untreated is also another consequence of peripheral neuropathy, a common complication of diabetes (Greenhalgh, 2003). Lower limbs, especially the feet, are particularly affected by these effects, since they are more prone to injury and therefore to chronic wounds. In addition to foot deformities, increased pressure on the soles of the feet, and excessive dryness, motor and sympathetic dysfunctions can result in cracks and small wounds that go unnoticed (Greenhalgh, 2003).

Sitagliptin phosphate, also known as Januvia®, is an oral diabetes medication. The compound inhibits dipeptidyl peptidase-4 (DPP-4), which is responsible for degrading glucagon-like peptide-1 (GLP-1), one of the hormones that regulate blood sugar levels. Sitagliptin blocks DPP-4 activity, preventing the breakdown of GLP-1, resulting in an increase in active GLP-1 levels in the bloodstream (Gallwitz, 2007). Other regulatory peptides such as glucose-dependent insulinotropic peptide (GIP) are also inactivated by DPP-4 via enzymatic cleavage (Nauck and El-Ouaghlidi, 2005). By specifically inhibiting DPP-4 instead of other DPP enzymes, sitagliptin prolongs the action of GLP-1 (Demuth et al., 2005).

A lipid-based transferosome is a rigid lipid bilayer or non-ionic surfactant monolayer vesicle that possesses flexibility, high deformability, and ability to respond to stress (Rajan et al., 2011). Despite their common use as drug delivery systems for skin applications, nanoparticles, liposomes, and nanosomes generally penetrate the stratum corneum (SC) and accumulate in the epidermis, but they cannot penetrate deeper layers of the skin, such as the dermis, or achieve effective systemic levels. It has been shown that small unilamellar liposomes have a greater ability to penetrate the skin compared to larger liposomes (Verma et al., 2003). Transferosomes are the most stable colloidal particles in liquid media, exhibiting the highest zeta potential (Van Zyl et al., 2019). The physical stability of transferosomes has also been demonstrated for up to three months at both 4 and 25°C (Hadidi et al., 2018). Transferosomes are created by modifying liposome lipid components with edge

activators (EA) or surfactants (Cevc, 1993). In addition to possessing greater elasticity than conventional liposomes, transferosomes are more able to penetrate through small pores and are less prone to bilayer damage than rigid liposomes (Habib et al., 2010). It is possible for transferosomes to penetrate through the stratum corneum by squeezing through the intercellular sealing lipids. In addition to following the natural water gradient through the epidermis, transferosomes have flexible membranes that minimize the chances of vesicle rupture once they are applied to the skin (Pandey et al., 2009).

The silver nanoparticle (AgNP) has a number of beneficial biological properties, including antibacterial, antiviral, antifungal, antioxidant, anti-inflammatory, anti-angiogenic, and antiplatelet effects. This makes them very useful as a preventative measure in diabetic chronic wounds and non-healing wounds (Lara et al., 2011). As a result of its biodegradability, biocompatibility, cellular binding capability, wound healing effects, and antimicrobial activity (Li et al., 2012), chitosan, which is derived from partially deacetylated natural chitin, is showing promising wound healing applications (Jiang et al., 2015). Numerous studies have reported different bioactivities of chitosan, including antimicrobial (Machul et al., 2015), antifungal (Vimala et al., 2010), antioxidant (Martínez-Gutierrez et al., 2012), antitumor (Gupta and Kumar, 2015), and wound healing properties (Ahmed et al., 2018). As an FDA-approved biomaterial for various biomedical applications, polyethylene glycol (PEG) exhibits biocompatibility, protein resistance, non-immunogenicity, non-toxicity, and good water solubility, as well as promoting the healing of chronic wounds in diabetics (Younes et al., 2014). Cross-linked polymer hydrogels have high water absorption capacities and possess attractive swelling properties that mimic a biomimetic environment (Li et al., 2012). As a result, a mixture of chitosan-PEG with silver nanoparticles, especially in a hydrogel form, shows promise as a dressing for diabetic chronic wounds. Various therapeutic agents can also be delivered to wound sites through the controllable biodegradability of hydrogels. A wide range of biological applications exists for hydrogels, including drug and gene delivery (Li et al., 2012), tissue repair (Huglin, 1989), biosensor development (Singh and Ray, 2000), and numerous others.

In this study, we used a Box–Behnken design to prepare and optimize a sitagliptin phosphate-containing transferosome hydrogel for enhanced transdermal delivery of the drug. Additionally, we investigated the morphology of the nanoparticles, and the FTIR spectra, DSC thermograms, and in vitro drug release kinetics of the transferosome hydrogel.

2. Materials and Methods

2.1 Materials and equipment

Sitagliptin phosphate was received as a gift sample from Glenmark. Streptozotocin was procured from Sigma Aldrich; Alloxan Monohydrate from SRL Laboratories;

Lipoid S 100 from Lipoid; and Tween 80 from Maya Chemtech. Chloroform, methanol, and ethanol used were of analytical grade. Rotary evaporator to prepare the transferosomes was manufactured by Medica Instrument Manufacturing Company. Ultrasonic probe sonicator used for reduction of suspension was manufactured by Sonics Vibracell. FTIR spectrometer used to generate infrared absorption spectrum of the drug was manufactured by Shimadzu (IR Affinity-1S). UV-Vis spectrophotometer used for generating calibration curve was a UV-Visible Perkin Elmer instrument with lambda 25 and UV range of 190 to 1100 nm. Particle size analysis and zeta potential analysis were carried out at NMIMS Central Instrumentation Laboratory, Mumbai, and RC Patel Institute of Pharmaceutical Education and Research, Shirpur. SEM, TEM, and AFM analyses were performed at Diya Labs, Mumbai.

2.2 Design and preparation of sitagliptin phosphate-loaded transferosomes

2.2.1 Preparation of transferosome nanoparticles

Before initiating transferosome preparation, sitagliptin phosphate was subjected to pre-formulation studies to test various physical and chemical properties such as colour, melting point, solubility, identification using FTIR spectroscopy, thermal study using DSC, and calibration using UV-Vis spectrophotometer and HPLC.

A flowchart of the method used for preparing the transferosomes is given in Figure 1. The rotary evaporation-sonication method was used for preparation of the transferosomes (El-Afify et al., 2018). Briefly, 75 mg of soy phosphatidylcholine and 25 mg of tween 90 were mixed in a solution of ethanol:methanol in a 5:5 ratio. 10 mg of sitagliptin phosphate was added to this solution. The solution was bath sonicated for 5 minutes and the contents were transferred to an RBF. The rotary evaporator was operated under low pressure at 75 rpm for 1.5 hours resulting in the formation of a thin film of the solution. This film was hydrated using 10 ml of phosphate buffer (pH 7.4) and once again rotated at 45 rpm for 1 hour at room temperature. The resulting suspension was probe sonicated for 10 mins at 40% power following which it was passed through a 0.45 µm membrane filter.

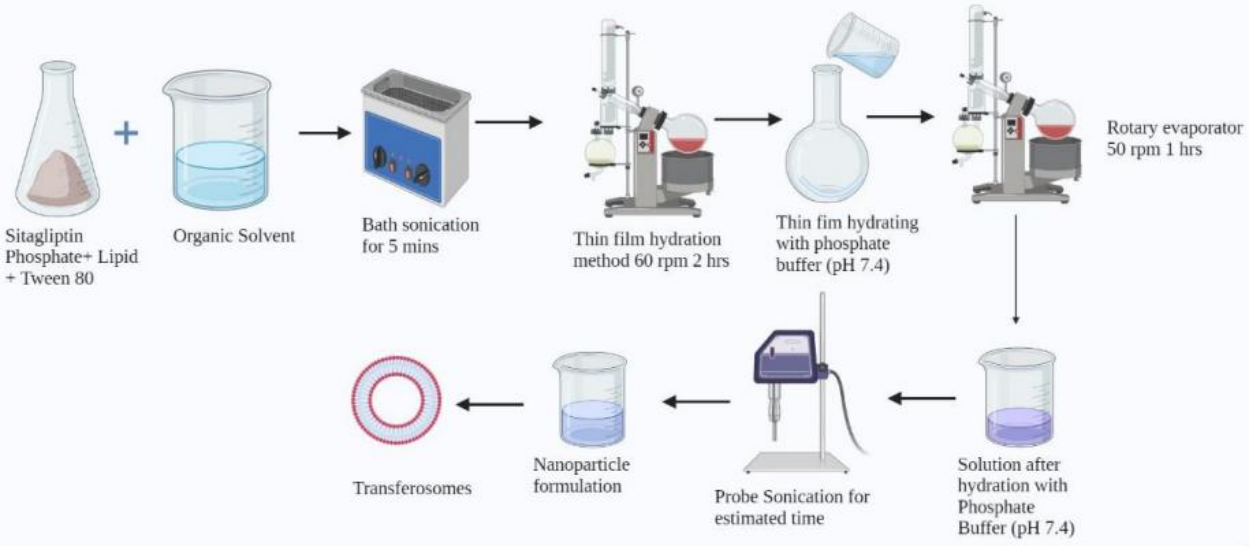

Figure 1: Flowchart illustrating the method of preparation of transferosome nanoparticles

2.2.2 DoE (Box Behnken Design) for optimization of transferosomes

The three main independent variables were phospholipid concentration (mg), surfactant concentration (mg), and sonication time (mins) that were adjusted at a low level (-1) and a high level (+1) according to a three-factor, two-level factorial design approach (2^3) for optimization. Preliminary tests were conducted to determine the values for the two levels for each of the three variables (Table 1). The dependent variables were entrapment efficiency (%) and vesicle size (nm). The mathematical model of the optimized batch was determined by preparing the design matrix using Design Expert 11 software. The trials were performed for 13 different combinations. The response matrix for the experimental design is given in Table 2.

Table 1: Parameters of independent variables and constraints of dependent variables for the design of transferosome nanoparticles

Independent Variables	**Levels**		
	Low (-1)	Medium (0)	High (+1)
Phospholipid concentration (mg)	70	75	80
Surfactant concentration (mg)	20	25	30
Sonication time (mins)	5	10	15
Dependent variables	Constraints		
Entrapment efficiency (%)	Maximize		
Vesicle size (nm)	Minimize		

Table 2: Factors and their responses for 13 trial formulations

		Factor 1	Factor 2	Factor 3	Response 1	Response 2
Std	Run	A: Phospholipid concentration (mg)	B: Surfactant concentration (mg)	C: Sonication time (mins)	Entrapment efficiency (%)	Vesicle size (nm)
7	1	70	25	15	72.77	102.64
8	2	80	25	15	61.24	90.23
5	3	70	25	5	65.21	97.23
13	4	75	25	10	67.88	104.09
6	5	80	25	5	56.66	89.48
2	6	80	20	10	76.33	94.33
4	7	80	30	10	84.22	111.23
3	8	70	30	10	79.88	108.66
12	9	75	30	15	75.5	95.69
10	**10**	**75**	**30**	**5**	**74.3**	**92.41**
9	11	75	20	5	69.22	103.84
11	12	75	20	15	57.8	106.27
1	13	70	20	10	59.22	88.24

2.3 In vitro characterization of transferosome nanoparticles

2.3.1 Particle size analysis

The mean diameter of transferosomes was calculated by measuring vesicle parameters such as vesicle size and polydispersity index (PDI) obtained from the Malvern Zetasizer. The samples were diluted 10 times in deionized water prior to each measurement. All measurements were performed in triplicates at 25 ± 0.1 ℃. PDI was used to assess size range.

2.3.2 Zeta potential analysis

Zeta potential was determined using dispersion technology software of the Malvern Zetasizer. Undiluted samples were transferred to plain folded capillary zeta cells and measurements were made at 25 ℃, dielectric constant 78.5, and dispersant viscosity 0.89 cP. All measurements were made in triplicates.

2.3.3 Determination of entrapment efficiency (%)

Entrapment efficiency was determined by centrifugation of the non-entrapped transferosomes at 10,000 rpm at 5 ℃ for 30 minutes. The supernatant was collected by decantation and examined using UV-Visible spectrophotometer at 267 nm in triplicates. Regression equation for EEy=0.0625x+0.0065 (Coefficient of correlation R^2=0.9978) was obtained by plotting the normal calibration curve of the drug

between absorbance (y-axis) and concentration (x-axis). The following equation was used to determine the entrapment efficiency of the transferosomes:

$$Percent\ entrapment\ efficiency = \frac{Amount\ of\ entrapped\ drug}{Amount\ of\ total\ drug} \times 100$$

2.3.4 FTIR spectroscopy

The ATR method was used to obtain the FTIR spectra of the drug alone and the transferosome nanoparticles. The successful formation of drug-encapsulated nanoparticles was determined by examining functional group peak shifts in the spectra as a result of encapsulation. All measurements were performed between 4000 cm^{-1} and 400 cm^{-1}.

2.3.5 Differential scanning calorimetry (DSC)

DSC thermograms of the drug and the transferosomes were obtained using Differential Scanning Calorimeter-800 (Perkin Elmer, USA) and thermal analysis was performed.

2.3.6 Microscopy

The transferosome nanoparticle suspension was diluted using ultrapure water and a droplet of the solution was placed on a glass coverslip. The coverslip was vacuum dried at 25 ℃ for 24 hours and subjected to AFM (Atomic Force Microscopy) under normal pressure and temperature while maintaining the instrument in a tapping state. The data thus obtained was analysed using AFM image analysis software. The transferosomes were also subjected to SEM and TEM to determine the surface morphology and size of the nanoparticles.

2.3.7 In vitro drug release study

A dialysis artificial membrane was hydrated with PBS (pH 7.4) overnight to ensure complete swelling to obtain a constant pore diameter. The donor and receptor compartments of the diffusion cell were separated using a cellulose dialysis membrane. 1 ml of transferosome suspension and 10 ml of PBS (pH 7.4) were added to the donor compartment under nonocclusive conditions. The diffusion cells were rotated on a magnetic stirrer at 100 rpm at 37 ± 0.5 ℃. Sink conditions were maintained by using 5 ml samples collected at predefined time intervals of 0 mins, 30 mins, 60 mins, 2 hours, 4 hours, 6 hours, 8 hours, and 12 hours, and they were replaced with an equal volume of fresh medium. The drug content was determined by analysing at 267 nm, and the calibration curve was generated to determine the amount of drug released from the nanoparticles over a 12-hour period. Using the drug release data, graphs for zero order kinetics, first order kinetics, Higuchi model, and Korsmeyer-Peppas model were prepared.

2.4 Preparation of transferosome hydrogel

A flowchart describing the method used for preparation of the transferosome hydrogel is given in Figure 2. The optimized batch of transferosome suspension (as determined by the BBD method) was used to prepare the hydrogel. Chitosan was soaked in 1% acetic acid and swirled on a hot plate for two hours to aid dissolution. The solution was filtered using Whatman filter paper and sodium hydroxide was added to neutralize the solution. The transferosome suspension was added to the chitosan solution, and 0.1 g of $AgNO_3$ was dissolved in it by swirling for 10 mins. A 1% PEG aqueous solution prepared in deionized water by mixing over a hot plate for one hour at 80 ℃ was added to the transferosome-chitosan solution and combined by stirring. 2% glutaraldehyde was added to the mixture to crosslink the two polymers. The resulting solution was taken in a petri plate and stored in a refrigerator.

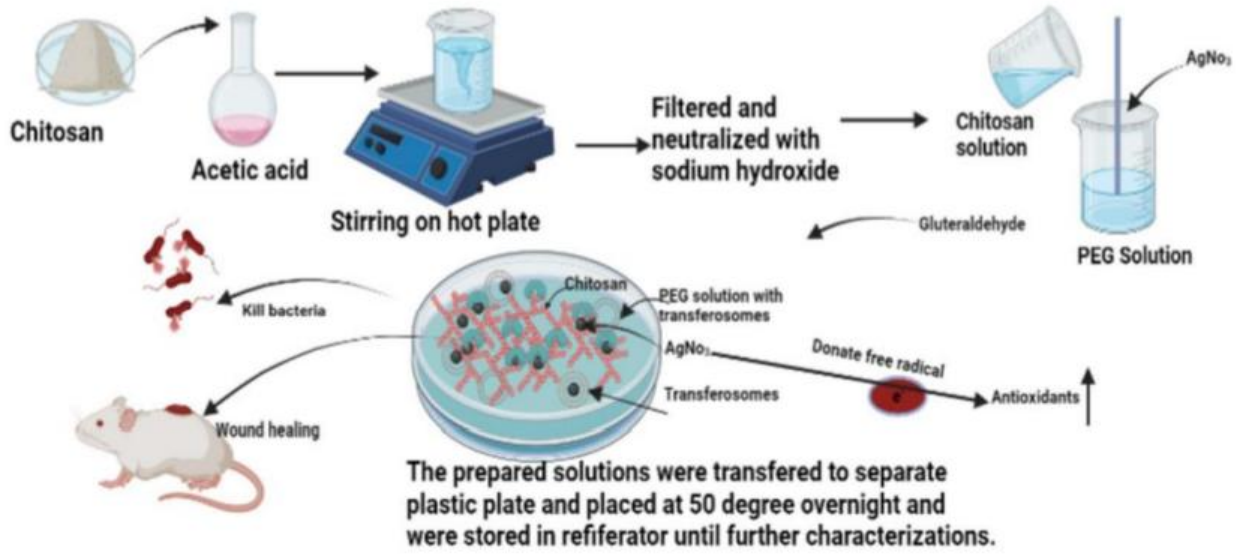

Figure 2: Flowchart illustrating the method of preparation of transferosome hydrogel

2.5 Characterization of transferosome hydrogels

2.5.1 Homogeneity and pH

Homogeneity of the hydrogel was examined visually for the presence of aggregates. pH was measured using pH meter. The acceptable pH limit for a topical gel is 7.0 to 7.4.

2.5.2 Drug content

10 ml methanol was added to the hydrogel and mixed until most of the gel was dissolved. The resulting solution was filtered using Whatman filter paper. 1 ml of the filtered solution was further diluted using 10 ml methanol and absorbance of the solution was recorded at 267 nm using only the gel solution as a blank.

2.5.3 Spreadability

Spreadability of the hydrogel was determined using an apparatus consisting of a wooden block with a pulley on one end. The hydrogel was placed at the centre of a glass slide and another glass slide was placed on the gel such that the hydrogel was sandwiched between the two glass slides. A weight of 100 g was placed on the top glass slide for 5 mins to expel the excess air. The increase in diameter of the hydrogel was measured and the spreadability index was calculated using the following formula:

$$Spreadability\ index = \frac{(Length\ of\ glass\ slide\ (cm)\ \times\ Weight\ applied\ (g))}{Time\ required\ for\ separation\ of\ slide\ (s)}$$

2.5.4 Swelling index

Pre-weighed hydrogels (transferosome hydrogels and only hydrogels) were briefly submerged in 250 ml PBS (pH 7.4) at room temperature until equilibrium was achieved. Water absorbed by the hydrogels was measured using an analytical balance at various timepoints (0.5, 1, 1.5, 2, 2.5, 3, 3.5, and 4 hours). The swelling index of the hydrogels was calculated using the following formula:

$$Degree\ of\ swelling\ (\%) = \frac{Wt.of\ wet\ hydrogel - Wt.of\ dry\ hydrogel}{Wt.of\ dry\ hydrogel} \times 100$$

2.5.5 Stability analysis

Stability analysis was carried out by assessing the visual appearance, pH, spreadability, and phase separation of the transferosome nanoparticles stored over a period of 3 months at 4 ℃ and 37 ℃.

2.5.6 In vitro diffusion study

Phosphate buffer (pH 7.4) was added to the 20 ml receiving container of a Franz diffusion cell. A determined amount of 5 mg of the sample was retained in the donor compartment following diffusion through the dialysis membrane. A 5 ml sample was obtained at regular time intervals over a period of 10 hours and the absorbance of the samples was measured at 267 nm.

3. Results and Discussion

In this study, sitagliptin phosphate-loaded transferosome nanoparticles were prepared and tested for their potential for transdermal delivery. Biocompatible and non-toxic materials, namely phospholipid and tween, were used to characterize the transferosome hydrogels.

3.1 Preparation and optimization of sitagliptin phosphate-loaded transferosome nanoparticles

The rotary evaporation-sonication method was used to prepare the transferosomes containing sitagliptin phosphate as it allows a thin film to be formed over a wide

surface area ensuring that the vesicles can be completely hydrated thereby increasing their entrapment efficiency (Jain et al., 2003). The preparation and optimization of transferosomes containing sitagliptin phosphate took place by the DoE method, Box Behnken design, and a three-factor two-level approach for a complete investigation of the effects and interactions of the independent variables namely phospholipid concentration (mg), surfactant concentration (mg), and sonication time (mins). The Box Behnken design has the advantage of requiring a minimum number of runs and therefore, it was chosen for our study (Qumbar et al., 2017). Data from 13 experimental runs was used to generate the design matrix, the outcomes of which are given in Table 2. The three-dimensional surface plots and the corresponding contour plots displaying the effects of the independent variables on entrapment efficiency and vesicle size are given in Figures 3 and 4 respectively. These figures aid the analysis of interactions between the factors and responses, along with the combined effects of two variables on each response. Table 3 provides the regression analysis results for the various factors and their responses. The quadratic nature of the interactions was confirmed by the fact that the standard error for coefficient had high values.

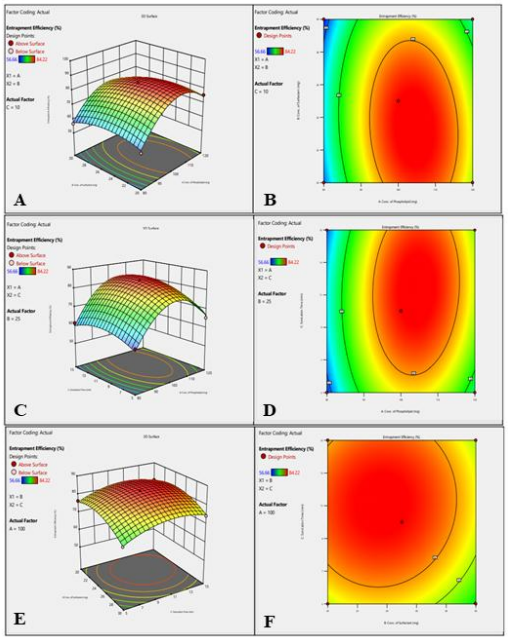

Figure 3: Surface plots (A, C, E) and contour plots (B, D, F) of the effects of the factors on entrapment efficiency. A and B represent the effect of phospholipid concentration and surfactant concentration on entrapment efficiency; C and D represent the effect of phospholipid concentration and sonication time on entrapment efficiency; E and F represent the effect of surfactant concentration and sonication time on entrapment efficiency

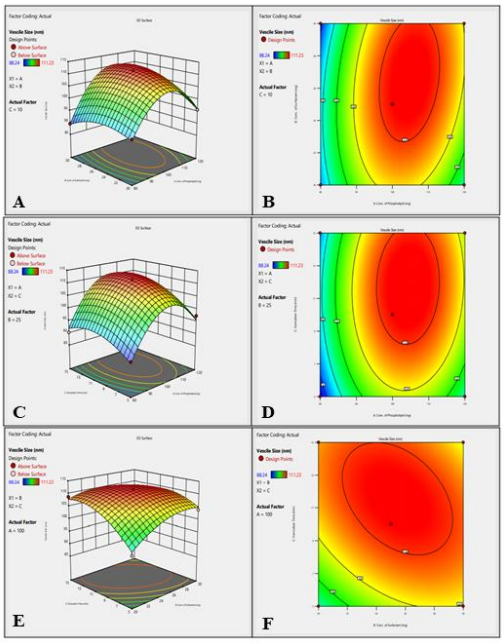

Figure 4: Surface plots (A, C, E) and contour plots (B, D, F) of the effects of the factors on vesicle size. A and B represent the effect of phospholipid concentration and surfactant concentration on vesicle size; C and D represent the effect of phospholipid concentration and sonication time on vesicle size; E and F represent the effect of surfactant concentration and sonication time on vesicle size

3.1.1 Effect of independent variables on entrapment efficiency

Entrapment efficiency refers to the quantity of drug that is retained within the transferosome nanoparticles. It is an important dependent variable that needs to be optimized for formulation of transferosomes. Phospholipids are generally used to prepare vesicular structures similar to liposomes as they are soluble in aromatic hydrocarbon or lipid carriers and insoluble in polar solvents. From the surface plots shown in Figure 3, there is an increase in entrapment efficiency with an increase in phospholipid concentration (Jangdey et al., 2017). Therefore, the combined effects of phospholipid concentration and surfactant concentration, and phospholipid concentration and sonication time on entrapment efficiency are direct; however, the combined effect of surfactant concentration and sonication time on entrapment efficiency is negligible.

According to the regression analysis (Table 3), the F-value of the model was 16.74 (p value = 0.0203; R^2 = 0.9805) indicating that the model is significant. The entrapment efficiency of the drug varied from 56.66 to 84.22% (Table 2). It is clear from Table 2 that both phospholipid concentration and surfactant concentration had a positive impact on entrapment efficiency. This may be attributed to a higher lipid content which is capable of encapsulating a higher quantity of the drug. This may also be attributed to the cosolvent effect of the phospholipid which increases the ability of the vesicles to encapsulate a higher amount of hydrophilic drug within their aqueous core thereby increasing the lipid-to-aqueous ratio within the vesicles. Our

results are in agreement with findings from other studies which indicate an increase in entrapment efficiency with an increase in lipid content (Habib and AbouGhaly, 2016; El-Gizawy et al., 2020). The high solubilizing effect of the surfactant may also contribute to an increase in entrapment efficiency (El-Zaafarany et al., 2010).

3.1.2 Effect of independent variables on vesicle size

The physicochemical properties of the transferosome nanoparticles play an important role in the delivery of a drug through the skin. From the surface plots and contour plots given in Figure 4, it is evident that the combined effect of surfactant concentration and sonication time reduces the vesicle size. This may be due to breakdown of the vesicle following sonication and an effect on the flexibility of the vesicle membrane upon exposure to the surfactant.

According to the regression analysis (Table 3), the F-value of the model was 18.38 (p value = 0.0178; R^2 = 0.9822) indicating that the model was significant. It has been suggested that vesicle size of less than 200 nm is ideal for transdermal delivery and bio-pharmaceutical performance (Hiruta et al., 2006). A small vesicle size aids in the diffusion of the drug (Rajan et al., 2011). The vesicle sizes for various formulations in the 13 trial runs is given in Table 2. The vesicle size of the transferosome nanoparticles varied from 88.24 to 111.23 nm. From table 2, it is clear that phospholipid concentration, surfactant concentration, and sonication time have a direct effect on vesicle size. It has been suggested that the amphiphilic surfactant is inserted into the lipid bilayer which results in increased cohesion between the polar regions of the membrane and enhanced hydration in the lipid layer. Therefore, a lower surfactant concentration would lead to insufficient hydration and lipid aggregation (Pathak et al., 2016). In our study, an increased surfactant concentration was used to reduce the vesicle size. It has previously been shown that an increase in hydrophilicity decreases the vesicle size (El-Afify et al., 2018). It is possible that using a hydrophilic surfactant reduces the free energy of the system thereby improving dispersion and reducing the vesicle size. It has also been reported that an increase in phospholipid concentration increases the vesicle size (Imam et al., 2015). This is because increasing the levels of phospholipids increase the particles available for creating the vesicles (Wang and He, 2009). Therefore, in our study, a lower phospholipid concentration was used to lower the vesicle size.

Table 3: Results of regression analysis for responses, entrapment efficiency and vesicle size, for determining fitting to the quadratic model

Response	p-value	Adjusted R^2
Entrapment efficiency	0.0203	0.9219
Vesicle size	0.0178	0.9288

Regression equations of the fitted quadratic model

Entrapment efficiency - $\mathbf{73.84 + 2.9225A + 0.445B + 1.77C + 1.83AB - 0.1AC - 0.42BC - 12.1675A^2 - 3.1625B^2 - 2.0475C^2}$

Vesicle size - $\mathbf{+111.23 + (4.91 \times A) + (1.57 \times B) + (3.02 \times C) + (2.83 \times AB) + (0.8550 \times AC) - (2.98 \times BC) - (12.25 \times A^2) - (3.56 \times B^2) - (4.39 \times C^2)}$

3.2 Optimization of transferosome nanoparticles

The response prediction method was used to choose the most optimized formulation from 13 trial runs as per the factorial design approach. The objective was to achieve the maximum entrapment efficiency and the minimum vesicle size. Based on the values obtained in the trial run, formulation 10 with a phospholipid concentration of 75 mg, surfactant concentration of 30 mg, and sonication time of 10 mins was found to be the most optimized formulation. This formulation had a vesicle size of 92.35 nm, an entrapment efficiency of 74.3%, and a zeta potential of -8.75 mV. The negative value of zeta potential ensures the stability of the particles and that the transferosomes will be easily able to permeate the skin topically (Pandit et al., 2020). The vesicle size and zeta potential of the optimized formulation are shown in Figures 5 and 6 respectively.

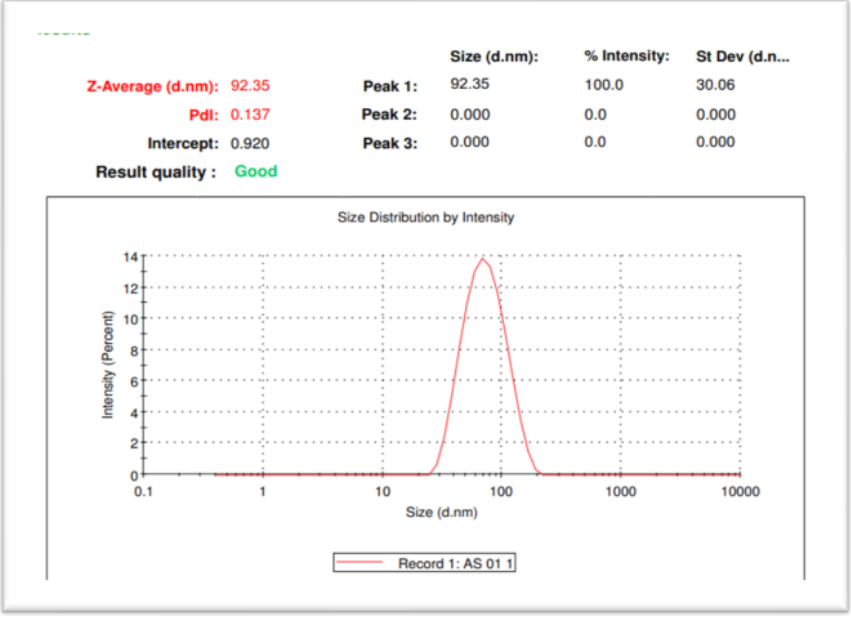

Figure 5: Vesicle size of the optimized formulation

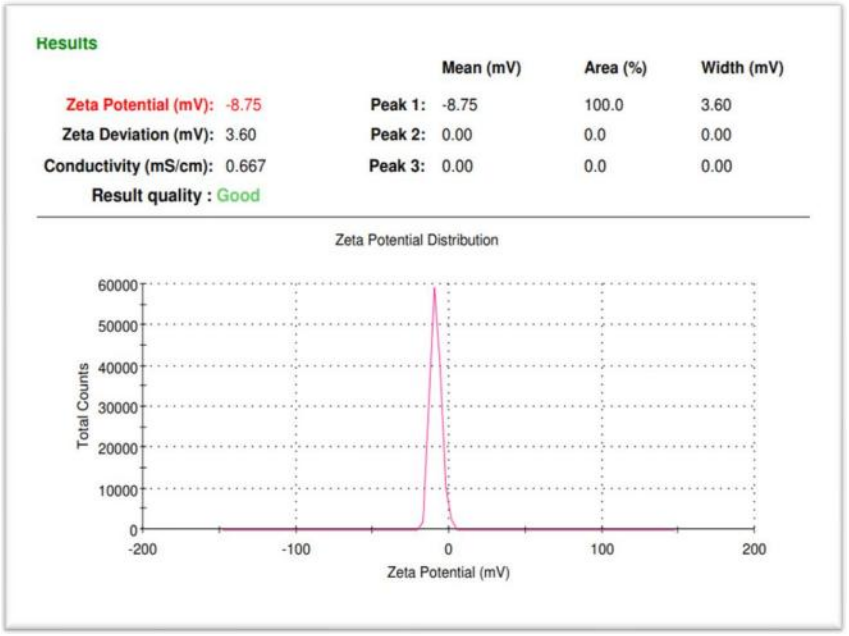

Figure 6: Zeta potential of the optimized formulation

3.3 Morphology of transferosome nanoparticles

3.3.1 Atomic Force Microscopy (AFM)

The 3-dimensional structure of transferosome nanoparticles obtained in AFM images is shown in Figure 7. In these images, the height of the nanoparticles was found to be variable indicating the presence of pores and channels on the particle surface. Skewness and kutosis values were present in the acceptable range.

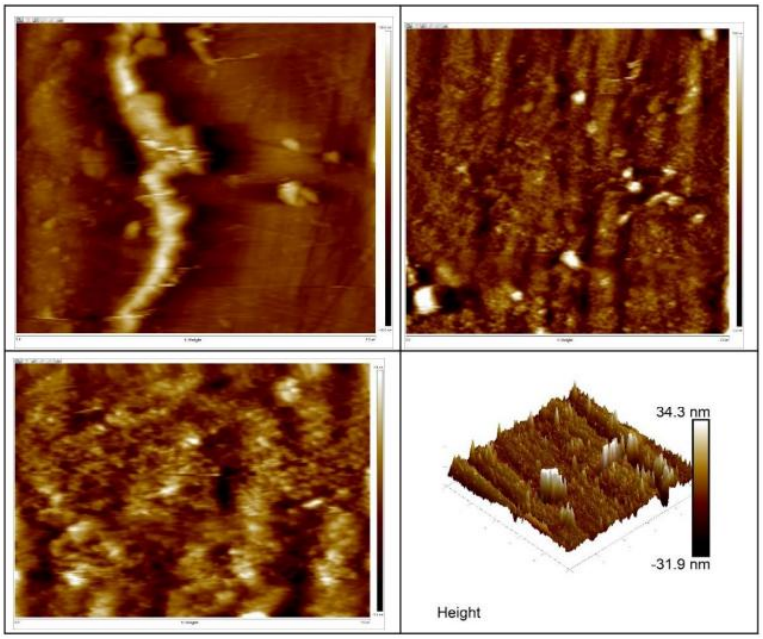

Figure 7: AFM images of the optimized transferosome nanoparticles

3.3.2 Scanning Electron Microscopy (SEM)

SEM images of the transferosome nanoparticles are shown in Figure 8. SEM analysis reveals that the particles are smooth, spherical and uniform in shape, and there is a clear separation of the particles as revealed by the value of the zeta potential. When a thin lipid film is hydrated, it tends to form spherical or oval vesicular structures to achieve thermodynamic stability in the system by reducing its free energy (Yusuf et al., 2014).

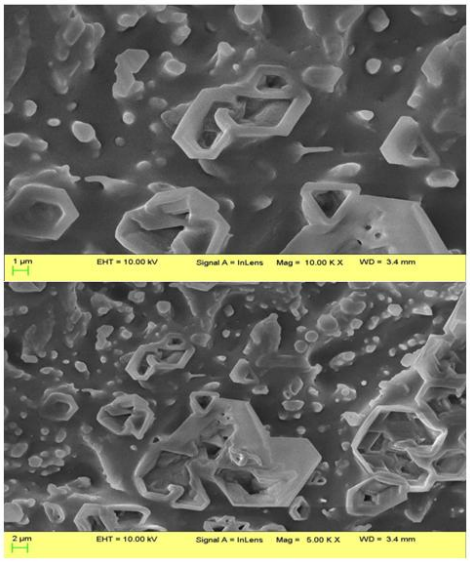

Figure 8: SEM images of optimized transferosome nanoparticles

3.3.3 Transmission Electron Microscopy (TEM)

TEM images of the transferosome nanoparticles are shown in Figure 9. Similar to SEM analysis, TEM images also revealed the presence of spherical and uniform transferosome nanoparticles in the formulation. Moreover, no disruptions or aggregations were found which indicate vesicular integrity.

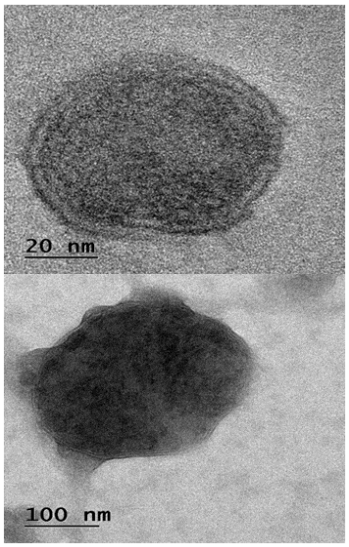

Figure 9: TEM images of optimized transferosome nanoparticles

3.4 Preparation of sitagliptin phosphate-loaded transferosome hydrogel

In this study, we developed chitosan-PEG hydrogels that were loaded with AgNPs to allow faster healing of wounds. PEG is a stabilizing agent, chitosan is a biodegradable and biocompatible carrier, and AgNP is an antibacterial agent. Several studies have reported the efficacy of hydrogels containing AgNPs for wound healing and antibacterial applications (Dhapte et al., 2014; Mekkawy et al., 2017; Masood et al., 2019). One limitation in this method of hydrogel preparation is that if AgNPs are not exposed to the environment, they cannot be released without an aqueous medium thereby limiting its antibacterial potential (Lodhi et al., 2010; Jadhav et al., 2016). In our study, the slow release of AgNPs has been used to enhance wound healing.

During the preparation of the hydrogel, it was observed that addition of PEG led to a reduction in AgNPs owing to the solubility of PEG in water (Diaz-Cruz et al., 2016). Addition of PEG also enhanced the stability of the silver nanoparticles which is important for maintaining prolonged biological activity (Pinzaru et al., 2018). The combination of AgNPs and chitosan helped in the formation of hydrogel, and addition of glutaraldehyde enhanced crosslinking thereby improving the stability of the hydrogel. Additionally, the presence of chitosan allowed the silver nanoparticles to freely interact with hydroxyl and amine groups present in the polymeric network. Finally, the hydrogel was subjected to swelling by treating it at low temperature so that a porous hydrogel with an even distribution of silver nanoparticles was formed.

3.5 In vitro characterization of transferosome hydrogel

3.5.1 pH

The pH of formulations that are intended for topical applications to the skin is important, as increased acidity or basicity of the formulation can alter the skin's natural environment (Basha et al., 2013). The pH value of the transferosomal gel formulation was found to be between 7 and 7.4, which is the acceptable range for avoiding skin irritation (Qushawy et al., 2018).

3.5.2 Drug content

The analysis of drug content is important as it reveals the uniformity in the distribution of the drug within the hydrogel. The transferosome gel formulation gave an absorbance of 0.627 at 267 nm; therefore, the drug content was calculated to be 99.28%. This indicates that the drug content was good and its distribution was uniform and consistent within the hydrogel.

3.5.3 Spreadability

Spreadability of the gel indicates its ability to be applied consistently so that it spreads easily over the applied area. It also directly impacts the therapeutic

efficiency of the formulation (Al-Suwayeh et al., 2014). The spreadability of the drug was found to be 14.56 ± 0.16 gcm/s, which is considered to be the optimum range for the drug.

3.5.4 Swelling index

Swelling tests were conducted for hydrogel formulations with and without a cross-linker. Figure 10 shows a plot between the swelling ratio (%) (y-axis) and the time (hours) (x-axis). It is evident that hydrogels without a cross-linker demonstrated greater swelling than hydrogels with a cross-linker indicating that the cross-linker attributes strength to the hydrogel and regulates its burst release. In this case, silver nanoparticles bind to the oxygen of the hydroxyl group and nitrogen of the amine group contributing to the crosslinking of the structure thereby lowering its capacity to absorb water and swelling ability (Ostrowska-Czubenko and Gierszewska-Druzynska, 2009). Also, as the polymer concentration increases, its ability to swell also increases as there are more free spaces available in the hydrogel. The swelling capacity of the hydrogel contributes to its use in wound healing and antimicrobial applications.

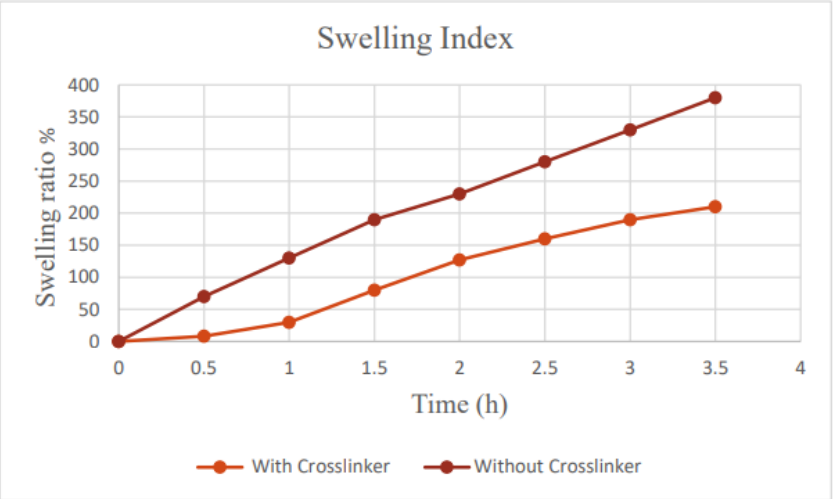

Figure 10: Swelling index of the optimized transferosome hydrogel with and without cross-linker

3.5.5 Stability

The parameters of visual appearance, pH, spreadability, and phase separation were evaluated over a period of 90 days at 4 ℃ and 37 ℃ (Table 4). No significant changes were found in the values at different temperatures and timepoints indicating the physical and chemical stability of the transferosome hydrogels.

Table 4: Stability studies of the optimized transferosome hydrogel

Parameters	**4 ℃**				**37 ℃**			
	Day 1	Day	Day	Day	Day 1	Day	Day	Day

		30	60	90		30	60	90
Visual appearance	No colour change	No colour change	No colour change	No colour change	No colour change	No colour change	Slight change	Colour fade
pH	7.4 ± 0.18	7.42 ± 0.21	7.47 ± 0.15	7.5 ± 0.18	7.4 ± 0.1	7.38 ± 0.14	7.32 ± 0.12	7.28 ± 0.22
Spreadability (gcm/s)	14.56 ± 0.7	13.22 ± 0.4	11.85 ± 0.2	10.18 ± 0.3	14.26 ± 0.3	12.75 ± 0.9	10.65 ± 0.1	10.25 ± 0.2
Phase separation	No	No	No	No	No	No	No	No

3.6 Drug-excipient compatibility studies

3.6.1 FTIR spectroscopy

FTIR spectroscopy was used to evaluate the drug-excipient interactions. The IR spectra of the sitagliptin phosphate-loaded transferosome nanoparticles and the transferosome hydrogel are given in Figure 11.

The spectrum of transferosomes was characterized by a band at 1637.56 cm^{-1} which signified C=C stretch of alkene group, a band at 3315.63 cm^{-1} which signified NH stretch of an amine group, and a band at 1045.42 cm^{-1} which signified a C-F stretch of an alkyl halide group.

The spectrum of the transferosome hydrogel was characterized by a band at 1641.42 cm^{-1} which signified C=C stretch of alkene group, a band at 3361.93 cm^{-1} which signified NH stretch of an amine group, and a band at 1074.42 cm^{-1} which signified a C-F stretch of an alkyl halide group.

This indicates that there is no chemical interaction between the drug and the excipients in the optimized transferosome formulation.

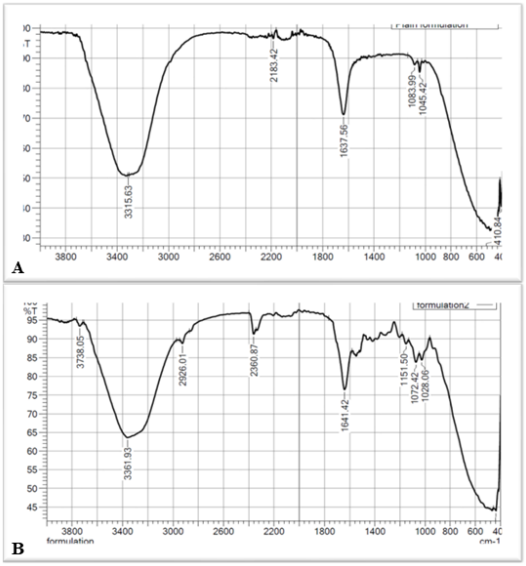

Figure 11: FTIR spectra of transferosome nanoparticles (A) and hydrogel (B) formulations

3.6.2 Differential Scanning Calorimetry (DSC)

DSC is an important calorimetric technique used to analyze solid-state interactions and determine the physical state of the drug present within the lipid vesicles (Shreya et al., 2016). The DSC thermograms of sitagliptin phosphate, phospholipid, and the physical mixture are given in Figure 12. The thermograms of sitagliptin phosphate and the physical mixture exhibited a sharp exothermic peak which was absent in the thermogram of phospholipid indicating that it had an endothermic reaction. This indicates that the drug and the physical mixture had the same transmission and that there was no interaction between the drug and the excipient.

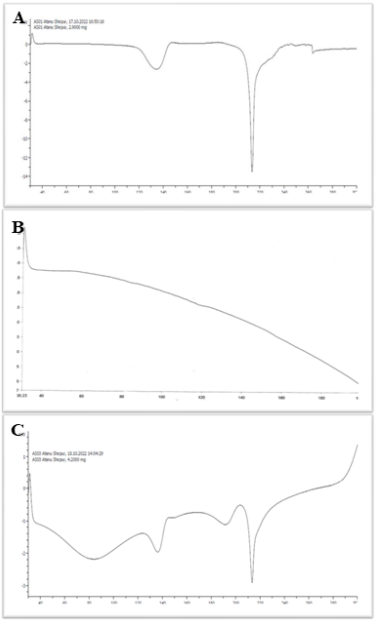

Figure 12: DSC thermograms of sitagliptin phosphate (A), phospholipid (B), and the physical mixture (C)

3.7 In vitro drug release kinetics

The in vitro drug release profile of the drug, drug-loaded transferosomes, and drug-loaded transferosome hydrogel is shown in Figure 13. From the figure, it is evident that a rapid release of the drug occurred within the first 30 minutes (97.43%); however, drug release time was prolonged for the transferosome nanoparticles (78.56% at 12 hours). This may be attributed to the time required for sonication of the materials for transferosome preparation which prolonged the drug release time. The drug release time for the hydrogel was 67.10% at 12 hours indicating a further prolongation of release time as the structure of the gel contributes to slow release of the drug. Various kinetic models such as Higuchi, first-order, Hixon-Crowell, Baker-Lonsdale, and Korsmeyer-Peppas were used to determine the mechanism of drug release. The Korsmeyer-Peppas model gave the best fit with a maximum R^2 value of

0.9988 for the nanoparticles and 0.9975 for the hydrogel indicating that the drug release mechanism was through diffusion and anomalous transport (Chauhan and Gulati, 2016). The results of our study demonstrate that the formulation provides a prolonged release profile as intended. Consequently, a sustained release subcutaneous drug reservoir has been created. It is possible to generate a localized, long-lasting impact at the site of application with such a system. This results in a reduction in the frequency of application, enhancing patient safety and comfort. Further, it eliminates the risks of infection, irritation, and increased pain associated with frequent wound dressing changes (Price et al., 2008).

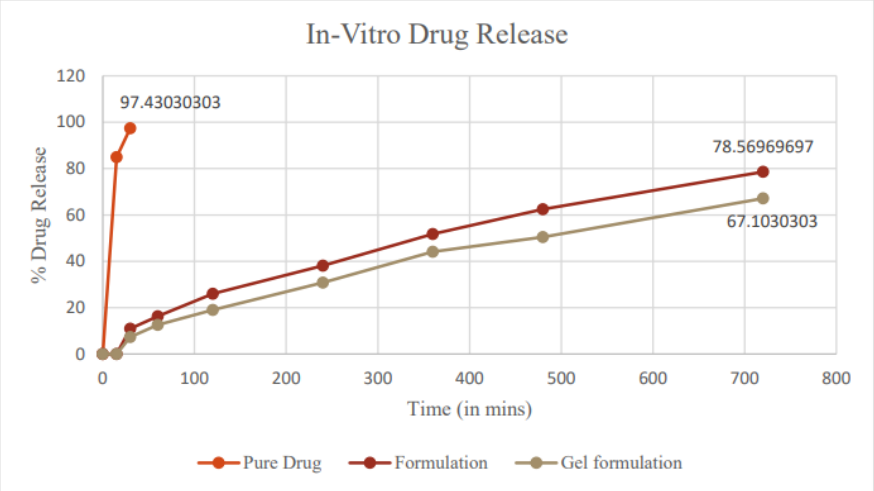

Figure 13: In vitro drug release kinetics

4. Conclusions

The aim of this study was to develop and assess a sustained-release nanogel containing sitagliptin phosphate for maintaining a continuous drug release concentration at the site of wounds/ulcers over an extended period. This approach aims to minimize exposure to foreign substances and promote timely healing, thereby reducing the risk of amputation and other adverse effects. The sustained-release microgel formulation was successfully prepared using a non-aqueous evaporation technique. Various parameters, including particle size analysis (92.35 nm), zeta potential analysis (-8.75 mV), entrapment efficiency (74.3%), and in-vitro drug release, were evaluated for both the drug formulation and gel formulation, demonstrating sustained drug release. The dissolution rate of all formulations was significantly sustained compared to the pure drug. The formation of nanoparticles was examined using SEM, TEM, and AFM, revealing spherical particles with smooth to rough surfaces. Microscopic images showed particle formation with minimal aggregation. Furthermore, a transferosomes-loaded hydrogel was prepared, and stability studies were conducted, yielding positive results. In conclusion, the formulation was successfully developed and evaluated, demonstrating its potential for sustained drug release pointing towards its potential use in clinical applications. Future studies could perform the in vivo characterization of the transferosome nanoparticles and hydrogel to establish its safety and efficacy in human subjects.